

Article

Synthesis of Bimetallic Nanoparticles of Cd₄HgS₅ by *Candida* Species

Araceli Romero-Núñez ¹, Gonzalo González ², Josué E. Romero-Ibarra ², Arturo Vega-González ³, Gustavo Cruz-Jiménez ⁴, Orlando Hernández-Cristóbal ⁵, Ramón A. Zárraga-Núñez ⁶, Armando Obregón-Herrera ¹, Everardo López-Romero ¹, Mario Pedraza-Reyes ¹ and Mayra Cuéllar-Cruz ^{1,7,*}

¹ Departamento de Biología, División de Ciencias Naturales y Exactas, Campus Guanajuato, Universidad de Guanajuato, Noria Alta S/N, Col. Noria Alta, Guanajuato C.P. 36050, Mexico; aracelitaromero@gmail.com (A.R.-N.); obregoa@ugto.mx (A.O.-H.); everlope@ugto.mx (E.L.-R.); pedrama@ugto.mx (M.P.-R.)

² Instituto de Investigaciones en Materiales, Universidad Nacional Autónoma de México, Circuito exterior S/N, Ciudad Universitaria, CDMX C.P. 04510, Mexico; joseggr@unam.mx (G.G.); jeromero@iim.unam.mx (J.E.R.-I.)

³ Departamento de Ingenierías Química, Electrónica y Biomédica, División de Ciencias e Ingenierías, Campus León, Universidad de Guanajuato, Guanajuato C.P. 36050, Mexico; avega@fisica.ugto.mx

⁴ Departamento de Farmacia, División de Ciencias Naturales y Exactas, Campus Guanajuato, Universidad de Guanajuato, Noria Alta S/N, Col. Noria Alta, Guanajuato C.P. 36050, Mexico; tavinio71@gmail.com

⁵ Laboratorio de Microscopía, Escuela Nacional de Estudios Superiores (ENES), Unidad Morelia, Universidad Nacional Autónoma de México, Antigua Carretera a Pátzcuaro No. 8701.Col. Ex Hacienda de San José de la Huerta, Morelia C.P. 58190, Mexico; ohernandez@enesmorelia.unam.mx

⁶ Departamento de Química, División de Ciencias Naturales y Exactas, Campus Guanajuato, Universidad de Guanajuato, Noria Alta S/N, Col. Noria Alta, Guanajuato C.P. 36050, Mexico; rzarraga@ugto.mx

⁷ Instituto de Química, Universidad Nacional Autónoma de México, Av. Universidad 3000, Ciudad Universitaria, Ciudad de México C.P. 04510, Mexico

* Correspondence: mcuellar@ugto.mx; Tel.: +52-473-732-0006 (ext. 8196)

Received: 19 December 2018; Accepted: 19 January 2019; Published: 24 January 2019



Abstract: In recent decades, it has been demonstrated that bimetallic nanoparticles (NPs) possess a number of advantages over monometallic NPs, as the combination of metals results in important changes to their physicochemical properties. Synthesis of bimetallic NPs can be achieved through a number of methods, yet there are serious difficulties in controlling these protocols. Biological methods based on the use of microorganisms exhibit important advantages over traditional methods, which makes the search for organisms such as bacteria, yeast and fungi endowed with these abilities an important task. In this context, it has been found that *Candida* species are able to biosynthesize monometallic NPs, but their ability to form bimetallic NPs has not been investigated. CdHgS is a bimetallic NP of special interest, as it has been found useful in a number of applications; however, its preparation by traditional methods poses certain limitations, and the ability to obtain it through biological procedures has never been demonstrated. With this in mind, the major purpose of this study is to evaluate whether several *Candida* species were able to synthesize bimetallic NPs of CdHgS in a Cd₄HgS₅ phase. To our knowledge, this is the first report on the biological synthesis of bimetallic NPs in *Candida* species.

Keywords: *Candida* species; monometallic nanoparticles; bimetallic nanoparticles; CdHgS NPs

1. Introduction

Nanoparticles (NPs) are of great importance in our daily lives. In vivo biosynthesis of NPs using organisms such as yeasts, bacteria and algae have demonstrated the availability to obtain these materials, as well as the possibility of removing hazardous elements from water, soil and industrial effluents [1]. Some advantages of biosynthetic approaches are their environmentally friendly, simple one-step protocols, their use of mild conditions and the production of water-stable homogeneous materials [2]. In vivo remediation is generally believed to be an advantageous water treatment approach that allows the generation of useful materials. However, for this technique to be successful, the existence of multiple chemicals/reagents in contaminated water has to be further investigated. Natural detoxification by microorganisms that immobilize, isolate and biomineralize toxic cations has been extensively studied regarding single-metal exposure. Most of these studies include bioremoval percentages and the mechanisms and kinetics of biomineralization. However, in the last decades it has been demonstrated that monometallic nanoparticles present disadvantages as compared to the bimetallic compounds. This is because the combination of two metals results in important changes in their physicochemical properties, such as unique size-dependent optical, electronic and catalytic effects that yield a better performance as compared to their monometallic counterparts [3–5]. Bimetallic NPs have a more important structure because of the presence of extra degrees of freedom, which depends on the thermodynamic properties of the system [4]. It is very important to understand the elaboration process of bimetallic NPs to obtain materials with specific properties and applications. A vast diversity of methods to synthesize monometallic NPs has been reported [4,6,7], but the controlled synthesis of bimetallic NPs is more difficult [4].

Several research teams have been successful in obtaining bimetallic NPs of varying composition using different protocols, such as electrochemical or chemical reduction, sputtering, sol-gel or hydrothermal methods and others [4]. Currently, biological systems such as bacteria, yeasts and fungi are being used for the synthesis of monometallic and bimetallic NPs because of their advantages as compared with other non-biological methods. For example, the biosynthesis of these NPs can be manipulated to affect size and shape by controlling culture parameters [1]. Hence, it is important to identify microorganisms capable of synthesizing bimetallic NPs with a high reproducibility and efficiency.

Candida species are of special interest, because these yeasts can be isolated from soil and aquatic habitats that have been contaminated with metals [8]. Moreover, *Candida* species are able to synthesize monometallic NPs such as CdS, PbS, HgS and HgCl₂ [8]. In spite of this, multimetal resistance of *Candida* has been barely studied. HgS and CdS NPs are among the monometallic NPs with different applications [8]. Conveniently, these two monometallic NPs exhibit similar crystallographic characteristics that allow them to synthesize bimetallic CdHgS NPs [9]. Synthesis of CdHgS NPs is of special biotechnological interest, as these NPs possess a better electric conductivity than monometallic CdS NPs [9] and are used in LED devices, quantum computing, optics and fluorescent devices, among others [10]. Bimetallic CdHgS NPs have been synthesized in vitro by distinct techniques [9], although it is known that some microorganisms are able to biosynthesize both monometallic and bimetallic NPs with higher efficiency.

In the present study, we demonstrate that *Candida* species are capable of forming monometallic NPs of CdS or HgS [8], suggesting that they might also be able to form bimetallic CdHgS NPs. This possibility was investigated using five species of the genus, namely, *Candida albicans*, *Candida dubliniensis*, *Candida glabrata*, *Candida krusei* and *Candida parapsilosis*, after exposure to a 1:1 mixture of Hg (II) and Cd (II). Both environmental and biosynthetic perspectives were evaluated using different techniques. Results indicate that susceptibility and metal uptake depended on the *Candida* strain, whereas distribution and crystal structure behavior of NPs were influenced by the metal.

2. Materials and Methods

2.1. Strains and Susceptibility Test

The strains of *C. albicans*, *C. dubliniensis*, *C. glabrata*, *C. krusei* and *C. parapsilosis* were clinical isolates from the collection of the Departamento de Microbiología, ENCB-IPN, México. They were grown in yeast peptone dextrose (YPD) (1% Bacto yeast extract, 2% Bacto peptone, 2% dextrose; 2% agar was added to solidify the media) at 28 °C for 24 h and stored at 4 °C. For the subsequent tests, fresh cultures of cells were cultured in YPD at 28 °C while being shaken at 200 rpm in an incubator model 311DS Labnet (Labnet International Inc., Woodbridge, NJ, USA). After 24 h, cultures of cells were adjusted to an optical density of 600 nm (OD_{600nm}) using a Genesys 20 Thermo Scientific spectrometer (Syngene, Cambridge, UK). Metal exposure was carried out by adding proper volumes of 0.1 M stock solutions of $Hg(NO_3)_2$ and $Cd(NO_3)_2$ to the inoculum to obtain a 1:1 metal mix, which was shaken at 28 °C for 48 h. For susceptibility tests, the total cation concentration was tuned from 0 to 4 mM. After 48 h at 28 °C and 200 rpm, an aliquot of each cell suspension was adjusted to an OD of 0.5 to prepare exponential dilutions in 96-well plates. Finally, each dilution was spotted in YPD-agar and incubated at 28 °C for 24 h. All used chemicals were provided by Bio-Rad (Hercules, CA, USA) and Sigma-Aldrich (Sigma-Aldrich, St. Louis, MO, USA).

2.2. Growth Curves and Metal Uptake

For growth curves and metal uptake studies, cultures were exposed to a 1:1 Cd^{2+} – Hg^{2+} mixture to obtain a total cation concentration of 1.0 mM, which was shaken at 200 rpm for 48 h at 28 °C. The cell uptake of heavy metal was calculated from the difference between the added and the remnant metal concentrations in the supernatant, as measured by atomic adsorption spectroscopy (PINACLE Perkin Elmer equipment, (PerkinElmer Inc., MA, USA). Cellular growth was monitored by OD_{600nm} measurements and run in duplicate.

2.3. Crystal Characterization

Identification and analysis of biogenic crystals were evaluated by electron microscopy techniques. Scanning electron microscope (SEM) was performed using a Carl Zeiss SIGMA-HDVP Field Emission Scanning Electron Microscope (Carl Zeiss NTS Ltd., Cambridge, UK), equipped with angle-selective backscatter (AsB) and Quantax Bruker energy-dispersive X-ray detectors (Bruker Nano GmbH, Berlin, Germany). Prior to observation, metal-exposed samples were washed with deionized sterile water, centrifuged several times and lyophilized at -48° , mounted on a carbon tape and covered with colloidal gold.

For transmission electron microscope (TEM) analysis, samples were fixed, embedded in resin and cut in ultrathin sections for observation. Fixation was performed by exposing the sample to 3% glutaraldehyde at 48 °C for 4 h, washing with sodium cacodylate buffer (0.1 M, pH 7.4) and gradually dehydrating with ethanol in steps of 10% to absolute ethanol, holding for 10 min at each ethanol concentration. Absolute ethanol was replaced by propylene oxide for infiltration, samples were placed in 1 mL of epoxy resin and dried at room temperature for 24 h doing repetitions with 25%, 50% and 75%. After this, polymerization was completed in plastic embedding molds filled out with 100% epoxy resin and stored at 60 °C for 36 h. The resulting blocks were cut in ultrathin sections 60 nm thick using an ultramicrotome (MTX-RMC, Boeckeler Instruments, Inc., Tucson, AZ, USA) and collected on TEM 300-mesh copper grids. Finally, carbon coating was applied to stabilize the ultrathin sections on the TEM grid surface. Transmission electron analysis was achieved using a JEOL JEM-ARM200F spherical aberration-corrected scanning transmission electron microscope (STEM) (JEOL USA Inc., Peabody, MA, USA) coupled with energy-dispersive X-ray spectroscopy (EDS, JEOL USA Inc., Peabody, MA, USA) and high-angle annular dark field (HAADF, JEOL USA Inc., Peabody, MA, USA) detectors. An accelerating voltage of 200 kV was used in TEM–HAADF mode. X-ray microanalysis was carried out and processed using AZTEC EDS software (Oxford Instruments plc, 2013). Micrographs were recorded

and analyzed with Gatan Microscopy Suite Software (DigitalMicrograph, Gatan Inc., Pleasanton, CA, USA) and HRTEM plugins (DigitalMicrograph, Gatan Inc., Pleasanton, CA, USA).

Emission spectrum analysis was performed using a Zeiss 880-NLO laser scanning microscope equipped with a Chameleon Vision II Ti Sapphire laser (Carl Zeiss NTS Ltd., Cambridge, MA, USA) with tuning wavelengths from 690 nm to 1060 nm. Chameleon laser power was operated at 1.0% and an open pinhole at 601.1. Observations were carried out in Zeiss Plan NEOFLUAR immersion objective 60X/1.3. Micrographs were acquired separating the emission into three channels, namely a blue or UV region (371–440 nm), a green/yellow region (450–550 nm) and a red region (560–730 nm). Punctual spectral emission was performed using a wavelength excitation of 800 nm and measuring emission intensity from 404 nm to 714 nm each 10 nm.

3. Results and Discussion

3.1. Susceptibility and Metal Uptake

Tolerance and uptake capacities of the five *Candida* species were evaluated regarding their susceptibility behavior when exposed to a mixture of the toxic cations Cd^{2+} – Hg^{2+} in a 1:1 metal ratio and a total concentration from 0.5 to 2.0 mM. For the sake of simplicity, the metal mixture was named after their elemental components Cd–Hg. As depicted in Figure 1, *C. albicans*, *C. glabrata* and *C. krusei* were able to resist a concentration of Cd–Hg as high as 1.0 mM, whereas *C. dubliniensis* and *C. parapsilosis* were susceptible to half this concentration.

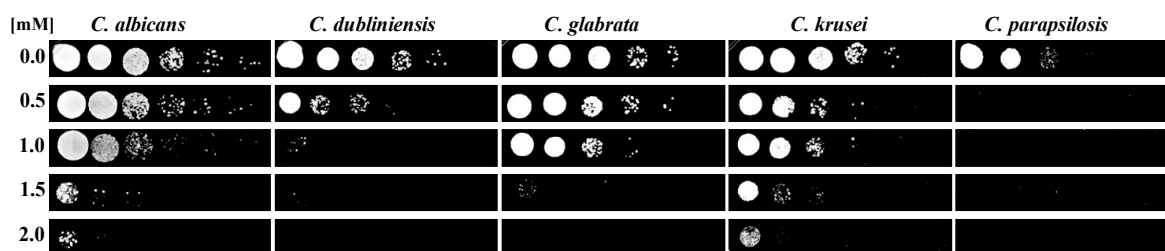


Figure 1. Susceptibility test of the five *Candida* species exposed to the Cd–Hg mixture ranging from 0 to 2.0 mM of total cation concentration. Cation ratio is fixed at 1:1.

Difference in susceptibility to toxic metals may have been due to the fact that species have adapted to habitats as different as the human body and soils and water contaminated with heavy metals [8,11–13]. It is worth noting that the most resistant *C. albicans*, *C. glabrata* and *C. krusei* are considered as the first species that adapted not only to contaminated soils and water, but also to different ecological niches where they developed mechanisms to cope with high concentrations of antifungals as well as reactive oxygen and nitrogen species produced by the human immunity system [14–16]. This does not seem to hold true for the more sensitive *C. dubliniensis* and *C. parapsilosis*.

As expected, susceptibility to a specific toxic agent depended on each *Candida* species and relied on each individual genetic background. Key factors in the bioaccumulation process were not only susceptibility, but also the ability to replicate in the presence of the metal mixture. This notion prompted us to monitor the growth of metal-exposed strains over the time. Representative growth curves of control and metal-exposed *C. albicans*, *C. glabrata* and *C. krusei* resisted 1 mM Cd–Hg are illustrated in Figure 2.

Growth of the exposed cells was inhibited by the Cd–Hg mixture. These results indicate that even when *C. albicans*, *C. glabrata* and *C. krusei* can resist 1.0 mM Cd–Hg (Figure 1), they do not duplicate (Figure 2)—most likely because they use their metabolisms to survive and not for the generation of new cells. These results are in accord with previous findings that indicate that cells go into homeostasis with toxic ions forming monometallic NPs of CdS or HgS without duplication [8].

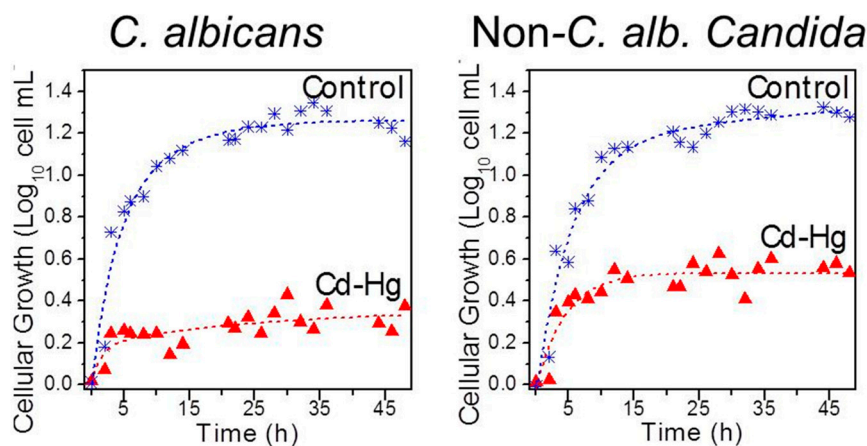


Figure 2. Growth curves of *Candida albicans* and representative non-*C. alb.* *Candida* (*C. glabrata* and *C. krusei*) when exposed to 1.0 mM Cd–Hg mixture. Non metal-exposed samples are shown as controls.

Additionally, removal percentages of the toxic mixture by cells were measured directly from the supernatant of exposed samples by atomic adsorption spectroscopy (AAS) (Figure 3).

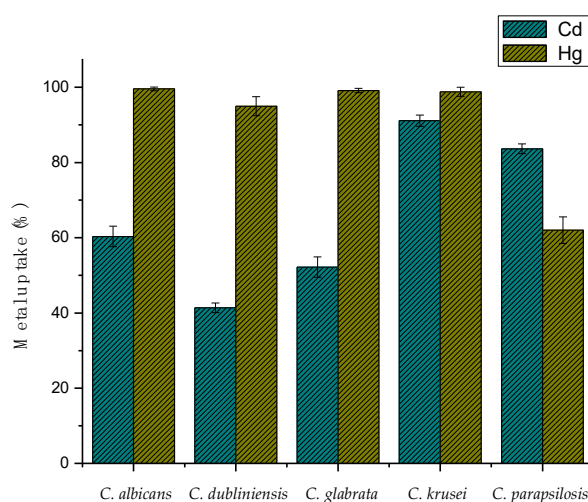


Figure 3. Cadmium and mercury uptake percentages of the five used *Candida* species when exposed to 0.5 mM Cd–Hg mixture during 48 h.

As depicted in Figure 3, cells incubated with the Cd–Hg mixture incorporated both cations. It has been described that Cd^{2+} interact with sulfhydryl groups of cysteine-rich, low molecular weight proteins known as metallothioneins, which inhibit some enzymes and thus play an important role in the toxicity of Cd^{2+} and Hg^{2+} [17], probably by facilitating their uptake by cells.

In summary, the yeast multi-metallic uptake represents a potential remediation technology for mercury combined with other heavy toxic metals. The process is driven by a community of mercury-resistant microorganisms selected by the metal toxicity in the host environment.

As resistance is often mediated by biomineralization, a biosynthetic response of exposed strains is next examined.

3.2. Identification and Characterization of Biosynthetic Materials

For the purpose of evaluating the effect of Cd–Hg on the cell structure of the five *Candida* species, exposed cells were observed by scanning electron microscopy (SEM). Photomicrographs show the formation of bright spots inside all *Candida* species (Figure 4).

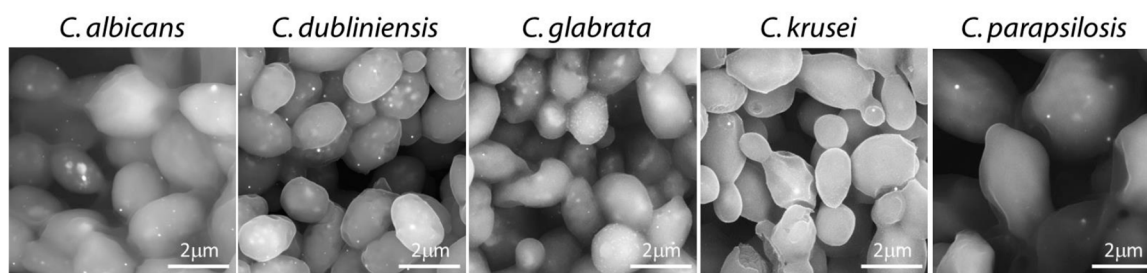


Figure 4. Scanning electron microscopy images of the five *Candida* strains exposed to the Hg–Cd mixture. Scale bar is indicated in each photomicrograph.

These correspond to bimetallic NPs of CdHgS (Figure 5). In a previous work we demonstrated the presence of similar bodies corresponding to nano- and micro-crystals in *Candida* species exposed to toxic elements [8]. To corroborate the nature of the bright spots, a qualitative analysis was carried out by energy-dispersive X-ray spectroscopy (EDS). As shown in Figure 5, EDS images revealed that these spots are formed by mercury, cadmium and sulfur (Figure 5), indicating that in the presence of Cd²⁺ and Hg²⁺, *Candida* species synthesize bimetallic NPs of CdHgS in their cytoplasm.

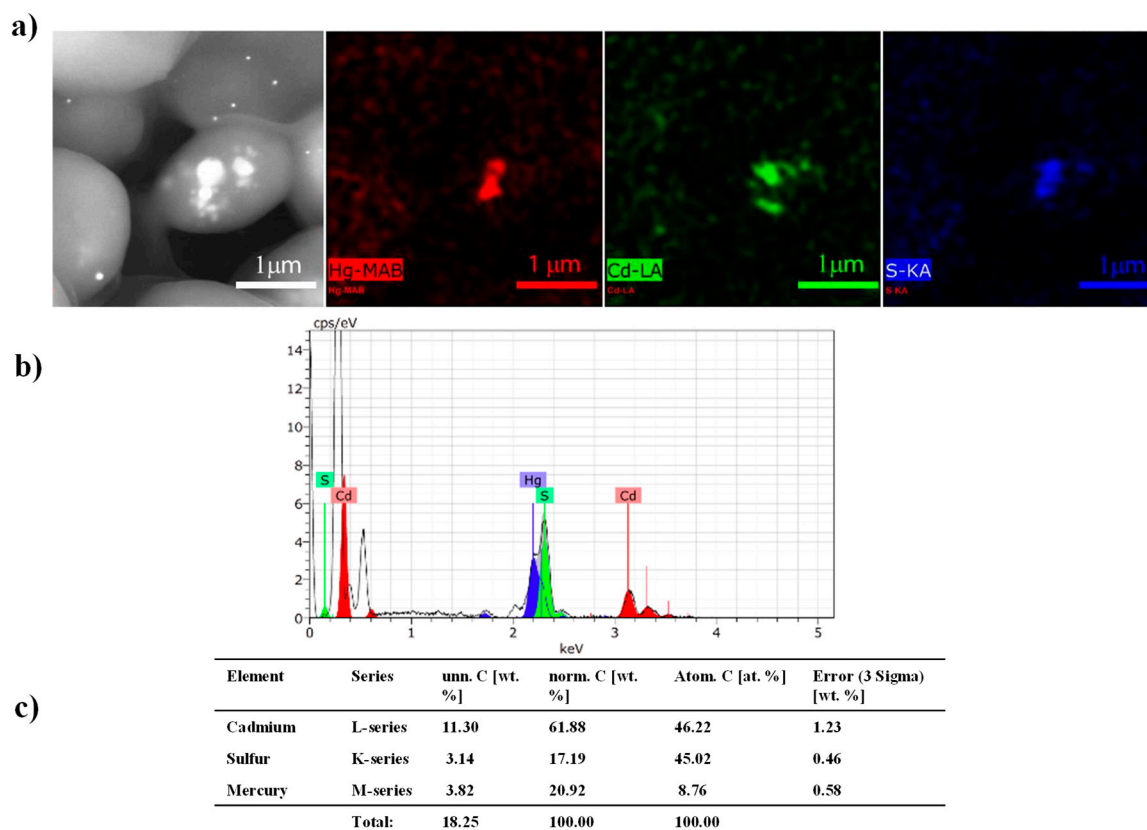


Figure 5. Formation of CdHgS nanoparticles (NPs) by *Candida* species in presence of the Cd–Hg mixture. (a) Electron image and elemental maps of Hg M α line, Cd L α line and S K α line; (b) qualitative analysis of the elements present in the formed compound; and (c) their corresponding quantification.

It has been proposed that formation of NPs inside the cell may occur as follows: (1) Toxic metals are transported into the cytoplasm by components that interact with this type of cations [18]. (2) Once in the cytoplasm, Cd²⁺ and Hg²⁺ bind to anions, inhibit transport and give rise to coordinated complexes with biomolecules and sulfhydryl groups that maintain them in the cytoplasm.

Another mechanism of Cd²⁺ uptake is by means of calcium channels, as both cations possess similar ionic radii [19,20]. In the case of Hg²⁺, it has been found that in methylation it forms

a methyl mercury complex that is structurally similar to methionine and thus transported as a neutral amino acid [21]. Another structural change observed in *Candida* cells exposed to Cd–Hg is the loss of their typical oval morphology and the presence of subsidences and deformations. In close concordance with these findings, we have observed that *Candida* cells exposed to stressing agents also lose their oval form [14].

To elucidate the chemical composition of the bimetallic NPs of CdHgS, the particles were analyzed by TEM. As illustrated in Figure 6, they exhibited a circular morphology with an approximate diameter of 10 nm. Zoom images depicted in Figure 6a–c show the size and appearance and the cell surroundings. The size of bimetallic NPs was within the average of 13.4 and 18.0 nm of the crystallite obtained by chemical synthesis [9].

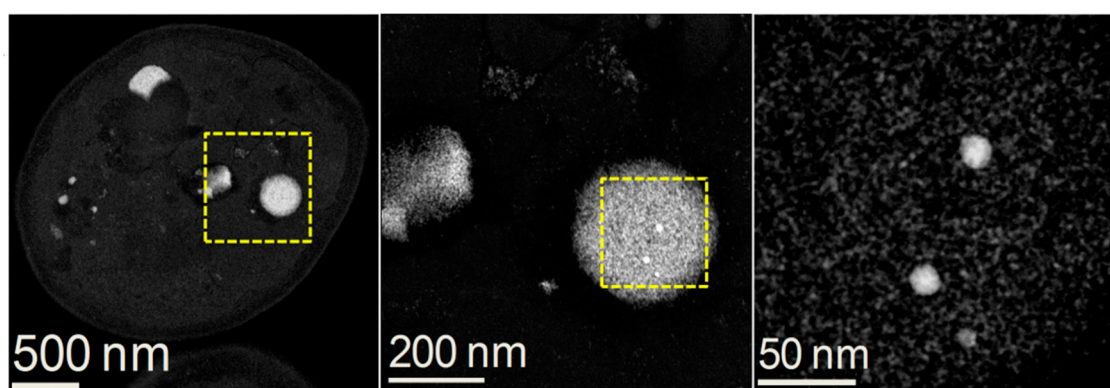


Figure 6. Ultrathin section's TEM–high-angle annular dark field (TEM–HAADF) analysis of representative Cd–Hg exposed *Candida*. Zooming into the bright material inside the cell revealed their nanometric nature. Dark field of the highest magnification is shown.

The EDS mappings in Figure 7 show the distribution of Hg, Cd and S in the proximity of bimetallic NPs of CdHgS. In order to reveal the crystal structure of CdHgS NPs, it was necessary to analyze them by high-resolution transmission electron microscopy (HRTEM) techniques.

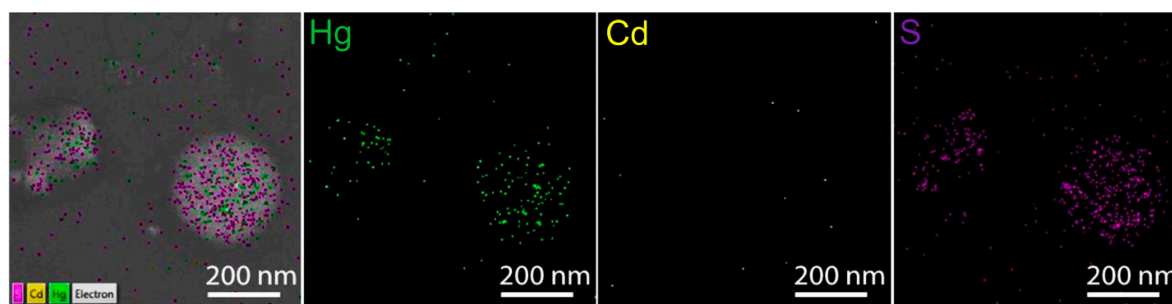


Figure 7. HAADF–STEM–energy-dispersive X-ray spectroscopy (EDS) analysis of the biosynthesized nanoparticles. Layered electron images and elemental maps of Hg, Cd and S are shown.

The HRTEM images provided evidence that NPs are constituted by conglomerates of smaller particles (Figure 8), and fast Fourier transform (FFT) diffraction patterns identified the Cd₄HgS₅ phase in close agreement with the elemental composition found by EDS. Figure 8b,c reveal a crystalline domain below 50 nm, with the FFT zone axis corresponding to [101] of an orthorhombic phase ($a = 10.752$ Å, $b = 12.566$ Å, $c = 7.255$ Å). As far as we know, such Cd₄HgS₅ nanoparticles have not been reported in *Candida* and complete other reports in literature that claim there is a wurtzite hexagonal phase [9] for other CdHgS nanoparticles.

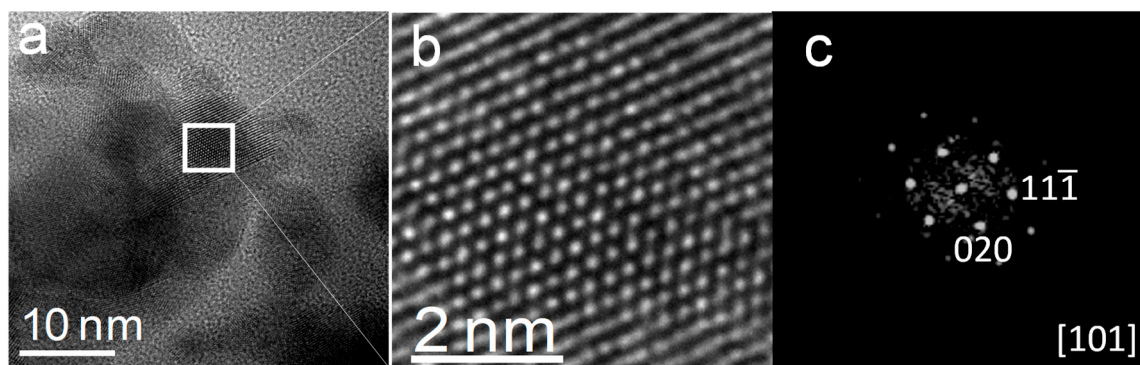


Figure 8. HRTEM images of Cd_4HgS_5 nanoparticles. (a) Agglomerated nanoparticles of about 10 nm; (b) higher magnification of the selected area in (a), clarifying the crystal structure oriented in the [101] zone axis as the corresponding (c) FFT shows.

4. Conclusions

To our knowledge, this is the first report on the biological synthesis of Cd_4HgS_5 bimetallic NPs, and in *Candida* species in particular. Our data indicate that these yeasts have mechanisms that allow them to achieve homeostasis for the Cd–Hg mixture. Cd_4HgS_5 NPs synthesized by *Candida* are very promising in terms of their potential applications in different areas. Experiments are in progress to explore these possibilities.

Author Contributions: Conceptualization, M.C.-C. and A.R.-N.; methodology, A.R.-N., G.G., J.E.R.-I., A.V.-G., G.C.-J., O.H.-C., R.A.Z.-N., A.O.-H., E.L.-R. and M.P.-R.; software, A.R.-N., G.G., J.E.R.-I. and O.H.-C.; validation, A.R.-N., G.G. and M.C.-C.; formal analysis, M.C.-C. and G.G.; investigation, A.R.-N., G.G., J.E.R.-I., A.V.-G., G.C.-J., O.H.-C., R.A.Z.-N., A.O.-H., E.L.-R. and M.P.-R.; writing—original draft preparation, A.R.-N. and M.C.-C.; writing—review and editing, M.C.-C., G.G. and E.L.-R.

Funding: This research was financed by Universidad de Guanajuato (Proyecto Institucional No. IDCIC-44/2018).

Acknowledgments: Araceli Romero-Núñez thanks Secretaría de Educación Pública for PRODEP postdoctoral support (Oficio No. 511-6/17-9480). Mayra Cuéllar-Cruz thanks the sabbatical leave support from SEP-PRODEP (Oficio No. 511-6/18-5929). Authors acknowledge the following colleagues: Lourdes Palma (INB-UNAM) for processing TEM samples, Diego Quiterio (IF-UNAM) for processing support, Paulina Lozano Soto Mayor (DCNE-UG) for SEM images, Iris V. Hernández Cervántes (Departamento de Química-UG) and C. Karina Sánchez Sánchez (DCNE-UG) for AAS assistance, Lino Sánchez (CINVESTAV Irapuato) for multi-wavelength measurements and Maritza Almanza-Villegas and Georgina Jiménez P. (DCNE-UG) for support in biological techniques.

Conflicts of Interest: The authors declare no conflict of interest.

References

1. Das, R.K.; Pachapur, V.L.; Lonappan, L.; Naghdi, M.; Pulicharla, R.; Maiti, S.; CleDon, M.; Dalila, L.M.; Sarma, S.J.; Brar, S.K. Biological synthesis of metallic nanoparticles: Plants, animals and microbial aspects. *Nanotechnol. Environ. Eng.* **2017**, *2*, 18. [[CrossRef](#)]
2. Ovais, M.; Khalil, A.T.; Islam, N.U.; Ahmad, I.; Ayaz, M.; Saravanan, M.; Shinwari, Z.K.; Mukherjee, S. Role of plant phytochemicals and microbial enzymes in biosynthesis of metallic nanoparticles. *Appl. Microbiol. Biotechnol.* **2018**, *102*, 6799–6814. [[CrossRef](#)] [[PubMed](#)]
3. Mallin, M.P.; Murphy, C.J. Solution-phase synthesis of sub-10 nm Au–Ag alloy nanoparticles. *Nano Lett.* **2002**, *2*, 1235–1237. [[CrossRef](#)]
4. Sharma, G.; Kumar, A.; Sharma, S.; Naushad, M.; Dwivedi, R.P.; AlOthman, Z.A.; Mola, G.T. Novel development of nanoparticles to bimetallic nanoparticles and their composites: A review. *J. King Saud Univ. Sci.* **2017**. [[CrossRef](#)]
5. Toshima, N.; Yonezawa, T. Bimetallic nanoparticles—Novel materials for chemical and physical applications. *New J. Chem.* **1998**, *22*, 1179–1201. [[CrossRef](#)]
6. Wang, A.; Liu, X.Y.; Mou, C.Y.; Zhang, T. Understanding the synergistic effects of gold bimetallic catalysts. *J. Catal.* **2013**, *308*, 258–271. [[CrossRef](#)]

7. Sau, T.K.; Rogach, A.L. Nonspherical noble metal nanoparticles: Colloid-chemical synthesis and morphology control. *Adv. Mater.* **2010**, *22*, 1781–1804. [[CrossRef](#)] [[PubMed](#)]
8. Cuéllar-Cruz, M.; Lucio-Hernández, D.; Martínez-Ángeles, I.; Demitri, N.; Polentarutti, M.; Rosales-Hoz, M.J.; Moreno, A. Biosynthesis of Micro- and Nano- Crystals of Pb (II), Hg (II) and Cd (II) Sulfides in Four *Candida* Species. A Comparative Study of in Vivo and in Vitro Approaches. *Microb. Biotechnol.* **2017**, *10*, 405–424. [[CrossRef](#)] [[PubMed](#)]
9. Lendave, S.A.; Karande, V.S.; Deshmukh, L.P. Optical and microstructural properties of chemically deposited mercury cadmium sulphide thin films. *Surf. Eng. Appl. Electrochem.* **2011**, *46*, 462–468. [[CrossRef](#)]
10. Yang, J.; Hu, Y.; Luo, J.; Zhu, Y.H.; Yu, J.S. Highly Fluorescent, Near-Infrared-Emitting Cd²⁺-Tuned HgS Nanocrystals with Optical Applications. *Langmuir* **2015**, *31*, 3500–3509. [[CrossRef](#)] [[PubMed](#)]
11. Hagler, A.; Mendonça-Hagler, L. Yeasts from marine and estuarine waters with different levels of pollution in the state of rio de janeiro, Brazil. *Appl. Environ. Microbiol.* **1981**, *41*, 173–178. [[PubMed](#)]
12. López-Archilla, A.I.; González, A.E.; Terrón, M.C.; Amils, R. Ecological study of the fungal populations of the acidic Tinto river in southwestern Spain. *Can. J. Microbiol.* **2004**, *50*, 923–934. [[CrossRef](#)] [[PubMed](#)]
13. Suihko, M.L.; Hoekstra, E.S. Fungi present in some recycled fibre pulps and paperboards. *Nordic Pulp Pap. Res. J.* **1999**, *14*, 199–203. [[CrossRef](#)]
14. Ramírez-Quijas, M.D.; Zazueta-Sandoval, R.; Obregón-Herrera, A.; López-Romero, E.; Cuéllar-Cruz, M. Effect of oxidative stress on cell wall morphology in four pathogenic *Candida* species. *Mycol. Prog.* **2015**, *14*. [[CrossRef](#)]
15. Cuellar-Cruz, M.; Briones-Martin-Del-Campo, M.; Canas-Villamar, I.; Montalvo-Arredondo, J.; Riego-Ruiz, L.; Castano, I.; Penas, A. High resistance to oxidative stress in the fungal pathogen *Candida glabrata* is mediated by a single catalase, Cta1p, and is controlled by the transcription factors Yap1p, kn7p, Msn2p, and Msn4p. *Eukaryot. Cell* **2008**, *7*, 814–825. [[PubMed](#)]
16. Serrano-Fujarte, I.; Lopez-Romero, E.; Reyna-Lopez, G.E.; Martinez-Gamez, M.A.; Vega-Gonzalez, A.; Cuellar-Cruz, M. Influence of culture media on biofilm formation by *Candida* species and response of sessile cells to antifungals and oxidative stress. *Biomed. Res. Int.* **2015**, *2015*, 783639. [[PubMed](#)]
17. Nordberg, M.; Nordberg, G. Toxicological aspects of metallothionein. *Cell. Mol. Biol.* **2000**, *46*, 451–463. [[PubMed](#)]
18. Nies, D.H.; Silver, S. Ion efflux systems involved in bacterial metal resistances. *J. Ind. Microbiol.* **1995**, *14*, 186–199. [[PubMed](#)]
19. Goyer, R.A. Response to Comments by Professor Duffus regarding Chapter 23, Toxic Effects of Metals. In *Cassarett and Doull's Toxicology*; McGraw Hill: New York, NY, USA, 2001; pp. 265–266.
20. Méndez-Armenta, M.; Ríos, C. Cadmium neurotoxicity. *Environ. Toxicol. Pharmacol.* **2007**, *23*, 350–358. [[PubMed](#)]
21. Pan-Hou, H.S.; Imura, N. Involvement of mercury methylation in microbial mercury detoxication. *Arch. Microbiol.* **1982**, *131*, 176–177. [[CrossRef](#)] [[PubMed](#)]

